RESEARCH ARTICLE

Subicular hypotrophy in fetuses with Down syndrome and in the Ts65Dn model of Down syndrome

Fiorenza Stagni[1]; Andrea Giacomini[1]; Marco Emili[1]; Beatrice Uguagliati[1]; Maria Paola Bonasoni[2]; Renata Bartesaghi[1] (ID) ; Sandra Guidi[1]

[1] Department of Biomedical and Neuromotor Sciences, University of Bologna, Bologna, Italy.
[2] Pathology Unit, Azienda Unità Sanitaria Locale, IRCCS, Reggio Emilia, Italy.

Abstract

Intellectual disability in Down syndrome (DS) has been attributed to neurogenesis impairment during fetal brain development. Consistently with explicit memory alterations observed in children with DS, fetuses with DS exhibit neurogenesis impairment in the hippocampus, a key region involved in memory formation and consolidation. Recent evidence suggests that the subiculum plays a unique role in memory retrieval, a process that is also altered in DS. While much attention has been devoted to the hippocampus, there is a striking lack of information regarding the subiculum of individuals with DS and DS models. In order to fill this gap, in the current study, we examined the subiculum of fetuses with DS and of the Ts65Dn mouse model of DS. We found that in fetuses with DS (gestational week: 17–21), the subiculum had a reduced thickness, a reduced cell density, a reduced density of progenitor cells in the ventricular zone, a reduced percentage of neurons, and an increased percentage of astrocytes and of cells immunopositive for calretinin—a protein expressed by inhibitory interneurons. Similarly to fetuses with DS, the subiculum of neonate Ts65Dn mice was reduced in size, had a reduced number of neurons and a reduced number of proliferating cells. Results suggest that the developmental defects in the subiculum of fetuses with DS may underlie impairment in recall memory and possibly other functions played by the subiculum. The finding that the subiculum of the Ts65Dn mouse exhibits neuroanatomical defects resembling those seen in fetuses with DS further validates the use of this model for preclinical studies.

INTRODUCTION

Individuals with Down syndrome (DS) are characterized by impairment in explicit memory, a cognitive function in which the hippocampal region is crucially involved (8,24,33). Defects in explicit memory are already evident in children with DS, suggesting malfunctioning of the hippocampal formation. Recent evidence shows that various structures of the hippocampal region of fetuses with DS are characterized by neurogenesis impairment and hypocellularity (14,15), which may account for the functional alteration in hippocampus-dependent memory functions observed in children with DS.

The hippocampal region is formed by the dentate gyrus, hippocampal fields CA3, CA2, and CA1, subiculum, presubiculum, and entorhinal cortex. Input signals from cortical and subcortical areas converge into the entorhinal cortex that redirects these signals to the dentate gyrus. These entorhinal projections are the first element of a circuit formed by the granule cells of the dentate gyrus, pyramidal neurons of field CA3, and pyramidal neurons of field CA1.

This circuit is classically known as the "trisynaptic circuit" (35). Field CA1 projects directly to the entorhinal cortex as well as to the subiculum. The subiculum itself gives origin to a parallel projection to the entorhinal cortex (22). Thus, the entorhinal cortex receives hippocampal signals through two major streams, one of which originates in field CA1 and the other one that originates in the subiculum (22). The entorhinal cortex sends processed hippocampal signals to the same cortical regions that are the origin of its major inputs. The circulation of signals along the entorhinal–hippocampal–entorhinal loop is considered to be fundamental for explicit memory. The term memory includes three basic processes, that is, memory formation, consolidation, and retrieval. While the role of the hippocampal fields in memory has been extensively studied and characterized, much less is known regarding the subiculum. In spite of the numerous connections of the subiculum within the hippocampal regions and various cortical and subcortical structures, little is known regarding its function. It has been thought that the subiculum

serves to amplify the hippocampal output and that it is involved in the processing of information of space, movement, and memory (25). More recently, based on fMRI studies in humans, it has been proposed that while the dentate gyrus and the hippocampal fields are involved in memory encoding, the subiculum is involved in memory retrieval (9). Confirming this hypothesis, more recent evidence suggests that two distinct microcircuits of the hippocampal region underlie the process of memory acquisition and recall. In particular, the projection from CA1 to the entorhinal cortex serves for memory formation and the CA1-subiculum-entorhinal circuit serves for memory retrieval (30). While inhibition of the subicular neurons during the training phase of the contextual fear conditioning test does not affect freezing during the retrieval phase, their inhibition during the retrieval phase reduces the amount of freezing (30).

Children with DS appear to be impaired in several aspects of memory, including recall memory (23). While much attention has been devoted to the hippocampal development in fetuses and adults with DS, there is a striking lack of information regarding the subiculum. The deficit in recall memory in DS is consistent with the hypothesis that the subiculum may develop abnormally in comparison with the euploid population. Thus, we deemed it of interest to examine the subiculum in fetuses with DS in order to establish whether it exhibits developmental alterations similarly to other structures of the hippocampal region. Mouse models are precious tools that allow dissecting mechanisms underlying a given pathology and to devise possible treatments. The Ts65Dn mouse is one of most widely used model of DS because it mimics various neuroanatomical and functional alterations of individuals with DS (17,27). The studies available so far have examined the dentate gyrus and hippocampus of the Ts65Dn mouse showing a constellation of anatomical and functional defects. Surprisingly, the subiculum, in spite of its role in memory functions, has been largely neglected and, to our knowledge, no study has examined the subiculum of the Ts65Dn mouse. A second goal of the current study was to examine the neuroanatomy of the subiculum of the Ts65Dn mouse, in order to fill this gap. We show here that the subiculum of fetuses with DS exhibits anatomical alterations similarly to other areas of the hippocampal region and that the subiculum of the Ts65Dn model is characterized by hypocellularity and reduced size similarly to the human subiculum.

METHODS

Study in fetuses with DS

Subjects

For this study, we used fetuses between 17 and 21 gestational weeks (GW). Brains were obtained after prior-informed consent from the parents and according to procedures approved by the Ethical Committee of the St. Orsola-Malpighi

Hospital, Bologna, Italy. Regulations of the Italian Ministry of Health and the policy of Declaration of Helsinki were followed. All fetuses derived from legal abortion and were collected with an average post-mortem delay of approximately 2 h. Six euploid fetuses with no obvious developmental or neuropathological abnormalities and six fetuses with DS were used (Table 1). These fetuses are the same used in previous studies (14,15). Trisomy was karyotypically proven from the results of genetic amniocentesis procedures. All cases were classical trisomy 21 (free trisomy). Autopsies were performed at the Institute of Pathology of the St. Orsola Malpighi Hospital (Bologna, Italy). The gestational age of each fetus was estimated by menstrual history and crown-rump length.

Histological procedures

Whole brains were fixed by subdural perfusion with Metacarnoy fixative (methyl alcohol: chloroform: acetic acid 6:1:1) injected through the anterior and posterior fontanelles. After 24–48 h the brains were removed, the region of the right hemisphere caudal to the mammillary bodies was dissected out, and coronally sectioned in order to obtain three to four blocks with a thickness of 2–3 mm. These blocks encompassed the brain region that stretches from the beginning to the end of hippocampal region. The blocks were post-fixed in 4% buffered formaldehyde for 5–7 days and embedded in paraffin according to standard procedures. The first block was cut so as to obtain, in addition to 8- or 12-μM-thick sections, five to six series of three to four 4- to 5-μM-thick sections, 200 μM apart. The 8–12-μM-thick sections were used for Nissl staining and the 4- to 5-μM-thick sections were used for immunohistochemistry.

Table 1. Cases of the present study. Abbreviations: CRL = crown-rump length; BW = body weight; F = female; M = male; n.a. = not available.

Case		Age (weeks)	Sex	CRL (cm)	BW (g)
Euploid fetuses					
C118	^§+*	17	M	13	180
C164	^§*	19	F	14	285
C27	^§*	20	F	17	230
C101	^+	20	M	15	340
C104	^+*	20	M	15	330
C178	^§*	21	M	n.a.	n.a.
Fetuses with Down syndrome					
C203	^§+*	18	F	14.5	210
C166	^§*	19	F	14	240
C133	^§*	20	M	16	300
C156	^+	20	M	17	385
C46	^§*	21	M	22	355
C77	^+*	21	F	17.5	300

List of the cases used in the present study. Cases labeled with ^ were used for stereology; cases labeled with § were used for NeuN and GFAP immunohistochemistry; cases labeled with + were used for CR immunohistochemistry; cases labeled with * were used for Ki-67 immunohistochemistry. Age refers to gestational age in weeks.

Nissl staining. Sections were deparaffinized in xylene, hydrated in graded ethanol to water, and stained with Toluidin Blue, according to the Nissl method, and differentiated in graded ethanols to xylene and cover-slipped.

Ki-67, NeuN, GFAP, and calretinin immunohistochemistry. Five to six sections were stained using monoclonal anti-Ki-67, from Novocastra Laboratories (dilution 1:500; clone MM1). Two to four sections were immunostained using monoclonal anti-NeuN (neuron-specific nuclear protein) from Chemicon International, USA (dilution 1:200; clone A60). Three to five sections were stained for glial fibrillary acidic protein (GFAP) using a monoclonal antibody from Sigma Chemical Co., USA (dilution 1:1600; clone G-A-5). Four to six sections were immunostained for calretinin (CR) using mouse anti-calretinin RTU, from Novocastra (dilution 1:300; clone 5A5). Sections were retrieved with citrate buffer pH 6.0 at 98°C for 40 minutes before incubation with their proper antibody. Sections immunostained for NeuN, GFAP, and calretinin were counterstained with Mayer's Hematoxylin.

Measurements

Unlike in the adult brain, the border of the fetal subiculum with field CA1 is poorly demarcated (2,19). For this reason, in the current study, we evaluated the subicular region that stretches for approximately 1000 μM from the pre-subicular border toward field CA1 (Figure 1C,D: region between the black and white arrowhead). Due to the scarcely identifiable border between the subiculum and field CA1, we could not quantify total cell number by using unbiased counting methods. For this reason, we quantified cell density instead of total cell number (see below).

Image acquisition. A light microscope (Leitz) equipped with a motorized stage and focus control system and a color digital camera (Coolsnap-Pro; Media Cybernetics, Silver Spring, MD, USA) were used to take bright field images. Measurements were carried out using the Image Pro Plus software (Media Cybernetics, Silver Spring, MD, USA).

Cell density and thickness of the subicular layers. The number of immunopositive and immunonegative cells counted in the sections processed for NeuN and calretinin immunohistochemistry (see below) was summed, divided by the size of the sampled area, and expressed as number of cells/mm^2. In Nissl-stained sections, the thickness of the pyramidal layer, and molecular layer of the subiculum was measured close to the border with the presubiculum in images taken at a final magnification of ×125.

Percentage of NeuN- and GFAP-positive cells. In sections processed for NeuN immunohistochemistry and counterstained with Mayer's Hematoxylin, the nuclei of neurons were heavily stained in brown, while cells that did not express NeuN exhibited a pale purple nuclear staining (Figure 3A). In sections processed for GFAP immunohistochemistry and counterstained with Mayer's Hematoxylin, the cytoplasm around the nucleus and the processes of astrocytes appeared stained in brown while the other cells exhibited only a pale purple nuclear staining (Figure 3B). In the series of sections processed for NeuN or GFAP immunohistochemistry, three snaps (size: 260 × 95 μM) per section were randomly acquired across the subiculum (objective: ×40, 0.70 NA; final magnification: ×500). In each acquired image, we counted all NeuN-positive and NeuN-negative cells and GFAP-positive and GFAP-negative cells. The number of NeuN- or GFAP-immunopositive cells was expressed as percentage of NeuN-positive or GFAP-positive cells over the total number of counted cells (immunopositive plus immunonegative cells). Since the percentage of cells that expressed NeuN plus that of the cells that expressed GFAP was lower than 100%, the percentage of cells with an undetermined phenotype was also evaluated.

Density and percentage of CR-positive cells. In sections processed for calretinin (CR) immunohistochemistry, images of the subiculum were acquired at a final magnification of ×312.5. In order to count CR-positive and CR-negative cells, 2 to 3 randomly chosen approximately rectangular areas (width: 60–100 μM; height: 250–600 μM) enclosing the whole thickness of the pyramidal layer of the subiculum were manually traced. All CR-positive and CR-negative cells within these areas were counted. The number of CR-positive and CR-negative cells was expressed in terms of (i) density per mm^2 and (ii) ratio of CR-positive vs. CR-negative cells. We additionally counted CR-positive cells in the ventricular zone (VZ) of the subiculum. The area of the VZ overlying the subiculum was first traced and all immunostained cells present within this area were counted. The number of counted cells was expressed as density per mm^2.

Density of Ki-67-positive cells. Proliferating cells were identified with immunostaining for Ki-67 (29,31). Ki-67-positive cells were counted in five to six sections in the pyramidal layer plus intermediate zone of the subiculum and in the VZ overlying the subiculum. For cell counting in the pyramidal layer plus intermediate zone, 2 to 3 randomly chosen approximately rectangular areas (width: 60–100 μM; height: 600–900 μM) enclosing the whole thickness of the pyramidal layer plus intermediate zone were manually traced. For cell counting in the VZ, the area of the VZ overlying the subiculum was first traced and all immunostained cells present within this area were counted. The number of counted cells was expressed as density per mm^2.

Study in Ts65Dn MICE

Colony and experimental protocol

Female Ts65Dn mice carrying a partial trisomy of chromosome 16 (27) were obtained from Jackson Laboratories (Bar Harbor, ME, USA) and maintained on the original genetic background by mating them with
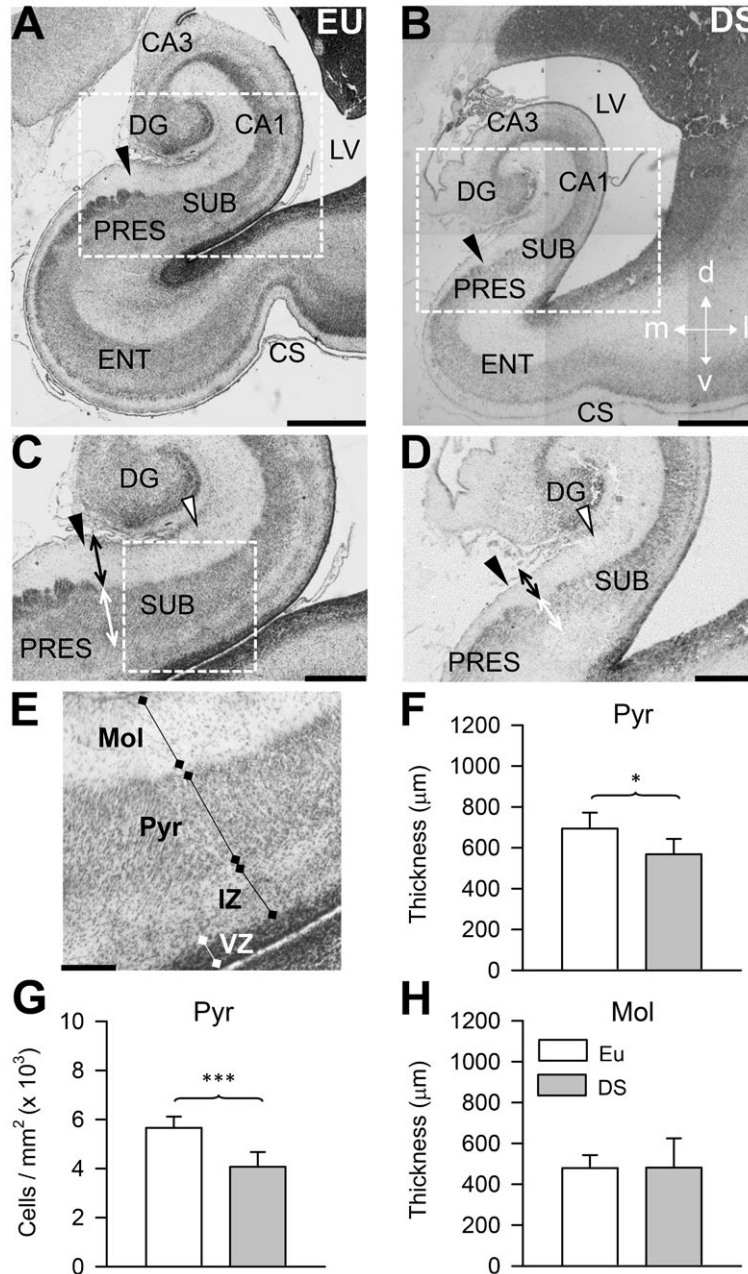
Figure 1. *Anatomy of the subiculum in euploid fetuses and fetuses with DS.* A–E. Representative images of Nissl-stained coronal sections across the hippocampal region of a euploid fetus (A, C, E; case 164) and a fetus with DS (B, D; case 166). Images in (C) and (D) are higher magnification of the boxed areas in (A) and (B), respectively. The image in (E) is a higher magnification of the boxed region in (C) and shows the layers of the subiculum, the ventricular zone, and the intermediate zone. The black arrowhead in (A–D) indicates the border between the subiculum and presubiculum. The region between the black arrowhead and the white arrowhead in (C) and (D) corresponds to the part of the subiculum examined in this study. The double-headed arrows in (C) and (D) indicate the location where the thickness of the molecular layer (black arrow) and pyramidal layer (white arrow) were measured. Calibration bar: A, B = 1000 µM; C, D = 500 µM; E = 200 µM. F–H. Thickness (F) and cell density (G) of the pyramidal layer, and thickness (H) of the molecular layer of the subiculum of fetuses with DS (n = 6) and euploid fetuses (n = 6). Values are mean ± SD. *$P < 0.05$; ***$P < 0.001$ (two tailed *t*-test). Abbreviations: CA1 and CA3 = hippocampal fields; CS = collateral sulcus; d = dorsal; DG = dentate gyrus; DS = Down syndrome; ENT = entorhinal cortex; EU = euploid; IZ = intermediate zone; l = lateral; LV = lateral ventricle; m = medial; Mol = molecular layer; Pyr = pyramidal layer; PRES = presubiculum; SUB = subiculum; v = ventral; VZ = ventricular zone.

C57BL/6JEi × C3SnHeSnJ (B6EiC3) F1 males. Animals were karyotyped as previously described (28). The day of birth was designed as postnatal day (P) zero. The animals had access to water and food *ad libitum* and lived in a room with a 12:12 h dark/light cycle. Experiments were performed in accordance with the Italian and European Community law for the use of experimental animals and were approved by Bologna University Bioethical Committee. All efforts were made to minimize animal suffering and to keep the number of animals used to a minimum. On P2, five euploid pups (three males and two females) and five Ts65Dn pups (two males and three females) received an intraperitoneal injection (150 μg/g body weight) of BrdU (Sigma) in 0.9% NaCl solution and were killed after 2 h.

Histological procedures

P2 mice were decapitated and their brain was removed. The brain was cut along the midline and fixed by immersion in Glyo-Fixx as previously described (6). Each hemisphere was embedded in paraffin and cut in series of 8-μM-thick coronal sections that were attached to polylysine coated slides.

BrdU immunohistochemistry. One out of every 20 brain sections was processed as previously described (12) and incubated overnight at 4°C with a primary antibody anti-BrdU (mouse monoclonal 1:100, Roche Applied Science, Mannheim, Germany). Detection was performed with a HRP-conjugated anti-mouse secondary antibody (dilution 1:200; Jackson Immunoresearch, West Grove, PE, USA) and DAB kit (Vector Laboratories, Burlingame, CA, USA). Sections were counterstained with hematoxylin.

Nissl-method. One out of every 20 brain sections was stained with Toluidine Blue according to the Nissl method.

Measurements

Image acquisition. A light microscope (Leitz) equipped with a motorized stage and focus control system and a color digital camera (Coolsnap-Pro; Media Cybernetics, Silver Spring, MD, USA) were used to take bright field images of sections processed for BrdU immunohistochemistry or Nissl-stained. Measurements were carried out using the Image Pro Plus software (Media Cybernetics, Silver Spring, MD, USA).

Stereology. In Nissl-stained sections encompassing the subiculum (n = 6–8 sections), the volume of the pyramidal layer of the subiculum, cell numerical density (N_v), and number (N) of neurons were estimated as previously described (6). The volume of the pyramidal layer of the subiculum (V_{ref}) was estimated (34) by multiplying the sum of the cross-sectional areas by the spacing T between sampled sections (160 μM). Cell numerical density was determined using the optical fractionator. Counting frames (disectors) with a side length of 30 μM and a height of 8 μM spaced in a 100 μM square grid (fractionator) were systematically used.

Cell nuclei were counted with a ×100 oil objective (1.4 NA). Cell nuclei intersecting the uppermost focal plane and intersecting the exclusion lines of the count frame were not counted. Calculation of CE of N_v gave values between 0.053 and 0.067.

The neuron density (N_v) is given by

$$N_v = (\Sigma Q/\Sigma \text{dis})/V_{dis}$$

where Q is the number of particles counted in the disectors, dis is the number of disectors, and V_{dis} is the volume of the disector. The total number (N) of cells was estimated as the product of V_{ref} and the numerical density (N_v).

$$N = N_v \times V_{ref}$$

Number of BrdU-positive cells. Images of serial sections processed for BrdU immunohistochemistry encompassing the subiculum (n = 6–8 sections) were taken at a final magnification of ×200. BrdU-positive cells were counted within the whole extent of the pyramidal layer plus molecular layer of the subiculum. The total number of BrdU-positive was estimated by multiplying the number of cells counted in the series of sampled sections by the section sampling frequency (ssf = 20). The mean number of cells per section was obtained by averaging the number of cells counted in all sampled sections.

Statistical analysis

Results are presented as mean ± standard deviation (SD). Statistical analysis was carried out using the two-tailed Student's *t*-test. A probability level of $P \leq 0.05$ was considered to be statistically significant.

RESULTS

Subicular region examined in fetuses with DS

The subiculum is interposed between field CA1 and the presubiculum. In the adult brain, the border between CA1 and subiculum is clearly recognizable because the relatively thin pyramidal layer of CA1 gives rise to a pyramidal layer that becomes progressively larger going toward the presubiculum. The adult subiculum is formed by three layers: the molecular layer that is the continuation of strata radiatum and lacunosum-moleculare of CA1, the pyramidal layer that contains the cell bodies of the principal neurons, and the polymorphic layer. In the fetal brain, a polymorphic layer is missing because immature neurons leaving the VZ traverse the developing alveus giving origin to a band of cells in the intermediate zone (Figure 1E). Unlike in the adult brain, the border of the fetal subiculum with field CA1 is poorly demarcated (2,19), whereas its border with the presubiculum is clearly recognizable (Figure 1A–D: filled arrowhead). For this reason, we examined here a

region of the subiculum proximal to the presubiculum. This region stretches for approximately 1000 μM from the presubicular border toward field CA1 (Figure 1C,D: white arrowhead).

Reduced cell density in the subiculum of fetuses with DS

Quantification of cell density in the pyramidal layer of the subiculum showed that while in euploid fetuses the density of cells was approximately 5600/mm^2, in fetuses with DS the density of cells was 4000/mm^2, with a difference of −28% (Figure 1G). The difficulty in recognizing the border of the subiculum with CA1 made it impossible to evaluate the subicular volume. Therefore, in order to obtain a rough estimate of possible size differences of the subiculum between fetuses with DS and euploid fetuses, we measured the thickness of the pyramidal layer of subiculum at its border with the presubiculum (Figure 1C,D: double-headed white arrow). We found that the subiculum of fetuses with DS had a reduced thickness in comparison with euploid fetuses (Figure 1F), with a difference of −18%. The reduced cell density in conjunction with the reduced thickness of the pyramidal layer suggest that fetuses with DS have an overall reduction in the number of cells populating the subiculum. An evaluation of the thickness of the molecular layer showed no differences between euploid fetuses and fetuses with DS (Figure 1H).

Reduced density of proliferating cells in the subiculum of fetuses with DS

Cell populating the pyramidal layer of the hippocampal fields and subiculum derive from neural progenitor cells (NPCs) in the VZ. NPCs leaving the VZ migrate across the intermediate zone and reach the pyramidal layer where they differentiate into neurons. Proliferating cells can be detected with Ki-67 immunohistochemistry, because this endogenous marker is expressed during all phases of the cell cycle. We previously found that in the VZ of the hippocampus of fetuses with DS, there were fewer proliferating NPCs, as assessed with Ki-67 immunohistochemistry, in comparison with euploid fetuses (14). In the current study, we specifically examined the density of Ki-67-positive cells in the VZ overlying the subiculum (Figure 2A,C) and of migrating Ki-67-positive cells in the intermediate zone and pyramidal layer of the subiculum (Figure 2A,B).

Results showed that in fetuses with DS, the VZ overlying the subiculum had fewer Ki-67-positive cells/mm^2 in comparison with euploid fetuses (−55%; Figure 2F). While in the VZ, there were numerous Ki-67-positive cells, in the intermediate zone and pyramidal layer only scattered Ki-67-positive cells could be detected. We found that in the intermediate zone plus pyramidal layer of fetuses with DS there were fewer (−49%) Ki-67-positive cells/mm^2 in comparison with euploid fetuses, although this difference was only marginally significant (Figure 2G). Taken together, these results suggest an impairment in the size of the

population of the actively dividing NPCs in the subicular VZ of fetuses with DS. Consistent with this reduction, fetuses with DS had a reduced density of migrating new cells in the marginal zone and pyramidal layer of the subiculum.

Reduced percentage of neurons and increased percentage of astrocytes in the subiculum of fetuses with DS

To establish the neuronal or astrocytic phenotype of the cells populating the subiculum we carried out immuno-histochemistry for NeuN, a marker of mature neurons, or GFAP, a marker of astrocytes. We found that fetuses with DS had a reduced percentage of NeuN-positive cells (Figure 3C) in comparison with euploid fetuses (−12%), but a larger percentage of GFAP-positive cells (+80%; Figure 3D). No significant differences were found in the number of cells with an undetermined phenotype (Figure 3E). These results show that in fetuses with DS NPCs exhibit an impairment in the acquisition of a neuronal phenotype in comparison with euploid fetuses, similarly to other structures of the hippocampal region (14).

Increased density of calretinin-positive neurons in the subiculum of fetuses with DS

Calretinin (CR), which is a marker of inhibitory GABAergic interneurons, has been shown to be expressed at early stages of embryonic (13) and fetal (4) brain development. In sections subjected to immunohistochemistry for CR, we found scattered CR-positive cells in the pyramidal layer of the subiculum (Figure 4C,D) (approximately 60 cells/mm^2 in euploid fetuses). Quantification of the density of CR-positive and CR-negative cells showed that fetuses with DS had more than twice CR-positive cells (+120%) in comparison with euploid fetuses, although this difference was only marginally significant (Figure 4F). As expected in view of their reduced density of cells in the pyramidal layer (Figure 1G), fetuses with DS had fewer CR-negative cells in comparison with euploid fetuses (Figure 4G). An evaluation of the percentage of CR-positive vs. CR-negative cells showed that in absolute terms, the percentage of CR-positive cells was extremely low, being approximately 1% in euploid fetuses. A comparison of DS and euploid fetuses showed that in fetuses with DS the percentage of CR-positive cells was significantly more than three times larger (+240%) than in euploid fetuses (Figure 4H).

An observation of the VZ lining the hippocampus, subiculum and parahippocampal gyrus showed that it contained numerous CR-positive cells. An example of CR-positive cells in the VZ of the subiculum is reported in Figure 4A,B. A comparison of the density of CR-positive cells in the VZ of the subiculum in DS and euploid fetuses showed that fetuses with DS had a slightly larger number of CR-positive cells per unit area than euploid fetuses, but that this difference was not significant (Figure 4E).
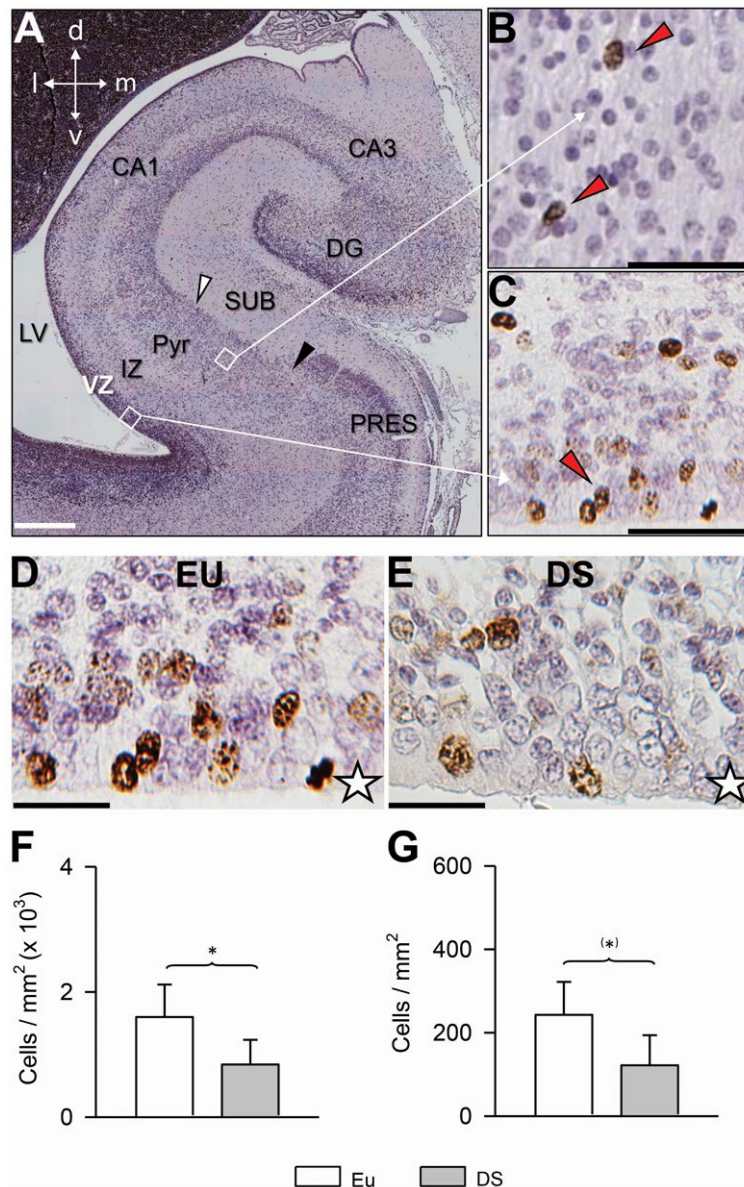
Figure 2. *Density of proliferating cells in the subiculum and subicular VZ in euploid fetuses and fetuses with DS.* **A.** Coronal section across the hippocampal region of a euploid fetus (case 104) immunostained for Ki-67 and counterstained with Mayer's haematoxylin. **B, C.** Higher magnification images of the regions enclosed by squares in (**A**), rotated approximately 45° counterclockwise. Cells immunostained for Ki-67 appear labeled in brown: see, for instance, the cells indicated by the red arrowheads. **D, E.** Examples of sections immunostained for Ki-67 and counterstained with Mayer's haematoxylin from the ventricular zone overlying the subiculum in a euploid fetus (**D**) and a fetus with DS (**E**). Images are from cases 104 (**D**) and 203 (**E**). The white star indicates the border of the VZ that faces the lateral ventricle. Calibration bar: A = 500 µM; B, C = 50 µM; D, E = 25 µM. **F, G.** Density of Ki-67-positive cells, expressed as number of cells/mm^2 in the ventricular zone (**F**) and pyramidal layer plus intermediate zone (**G**) of the subiculum of fetuses with DS (n = 5) and euploid fetuses (n = 5). Values are mean ± SD. (*)$P < 0.06$; *$P < 0.05$ (two tailed *t*-test). Abbreviations: CA1 and CA3 = hippocampal fields; d = dorsal; DG = dentate gyrus; DS = Down syndrome; EU = euploid; IZ = intermediate zone, l = lateral; LV = lateral ventricle; m = medial; PRES = presubiculum; Pyr = pyramidal layer; SUB = subiculum; v = ventral; VZ = ventricular zone.

Reduced cellularity and reduced number of proliferating cells in the subiculum of Ts65Dn mice

While numerous studies in Ts65Dn mice have concentrated on the dentate gyrus and hippocampal fields CA3 and CA1, there is a striking lack of data regarding the subiculum. For this reason, we deemed it of interest to obtain information regarding the subiculum of this model.

We found that in P2 mice, the subiculum was clearly recognizable and that its borders with field CA1 and
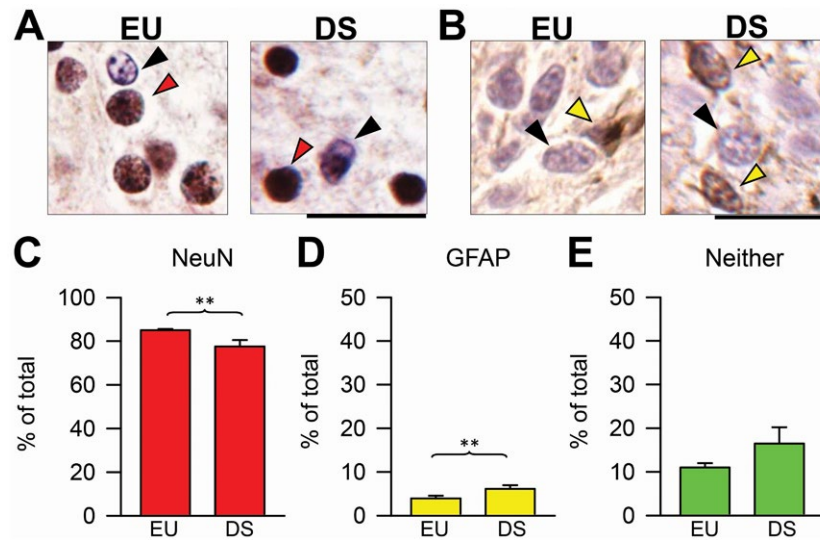
Figure 3. *Percentage of neurons and astrocytes in the subiculum of euploid fetuses and fetuses with DS.* **A.** Sections immunostained for NeuN and counterstained with hematoxylin from the subiculum of a euploid fetus (case 27) and a fetus with DS (case 46). The red arrowhead and the black arrowhead mark a NeuN-positive and a NeuN-negative cell, respectively. **B.** Sections immunostained for GFAP and counterstained with hematoxylin from the subiculum of a euploid fetus (case 178) and a fetus with DS (case 133). The yellow arrowhead and the black arrowhead mark a GFAP-positive and a GFAP-negative cell, respectively. Calibration bar: A, B = 20 µM. **C–E.** Percentage of NeuN-positive cells (**C**), GFAP-positive cells (**D**) and cells that did not express either NeuN or GFAP (**E**) over total cell number in the pyramidal layer of the subiculum of fetuses with DS (n = 4) and euploid fetuses (n = 3). Values are mean ± SD. **P < 0.01 (two tailed *t*-test). Abbreviations: DS = Down syndrome; EU = euploid.

cortical areas, respectively, were well delineated (Figure 5A–D: dotted lines). While in humans, the subiculum and the hippocampal formation (Cornu Ammonis) lie in the ventral part of the brain, the subiculum of mice has an overall dorsal location and stretches toward the ventral part of the brain only at caudal brain levels (Figure 5C,D).

Since the borders of the subiculum were clearly detectable, we could evaluate its volume and total cell number. We found that in Ts65Dn mice the subiculum had a reduced volume (−37%) in comparison with euploid mice (Figure 6C). An evaluation of cell density showed no difference between euploid and Ts65Dn mice (Figure 6C). Ts65Dn mice, however, had a significantly reduced total number of cells (−42%) populating the subiculum in comparison with euploid mice (Figure 6C), which is consistent with the notably reduced volume of the subiculum.

Mice are very immature at birth and numerous proliferating cells are still present in the brain of pups (16). In order to establish possible genotype-related differences in the number of proliferating cells in the subiculum, 2 h before sacrifice P2 mice were injected with BrdU, a marker incorporated by DNA during the S-phase of the cell cycle. We found that BrdU-positive cells were present in both the pyramidal layer and the molecular layer of the subiculum (Figure 6D,E). These cells were more concentrated in the molecular layer (see the higher magnification image in Figure 6D), suggesting that this layer may be their final destination. We found that Ts65Dn mice had fewer proliferating cells than euploid mice in terms of both total cell number (Figure 6F) and mean number of cells per section (Figure 6G).

DISCUSSION

The subiculum of fetuses with DS exhibits numerous neuroanatomical alterations

We found that the subiculum of fetuses with DS has a reduced thickness and a reduced cell density in comparison with euploid fetuses. Cells populating the subiculum and hippocampus derive from the VZ of the temporal horn of the lateral ventricle. An analysis of the density of Ki-67-positive cells in the VZ overlying the subiculum showed that fetuses with DS had significantly fewer proliferating NPCs than euploid fetuses. Neuroblasts born in the VZ retain mitotic capacity during their migration to their final destination. Accordingly, we found scattered Ki-67-positive cells in the pyramidal layer of the subiculum. Consistently with the reduced proliferation potency of NPCs in the VZ, fetuses with DS had a marginally reduced density of migrating neuroblasts in the pyramidal layer of the subiculum. The current analysis of Ki-67-positive cells represents a snapshot of the proliferation potency at mid-gestation. The reduced density of Ki-67 positive cells observed at this time point suggests that in fetuses with DS there is a proliferation defect that can be traced back at earlier gestational stages. This defect can account for the reduced cell density observed in the subiculum of fetuses with DS.

An important issue regards the phenotype of cells populating the DS brain. We found here that in both euploid fetuses and fetuses with DS most of the cells populating the subiculum were neurons and that much fewer cells
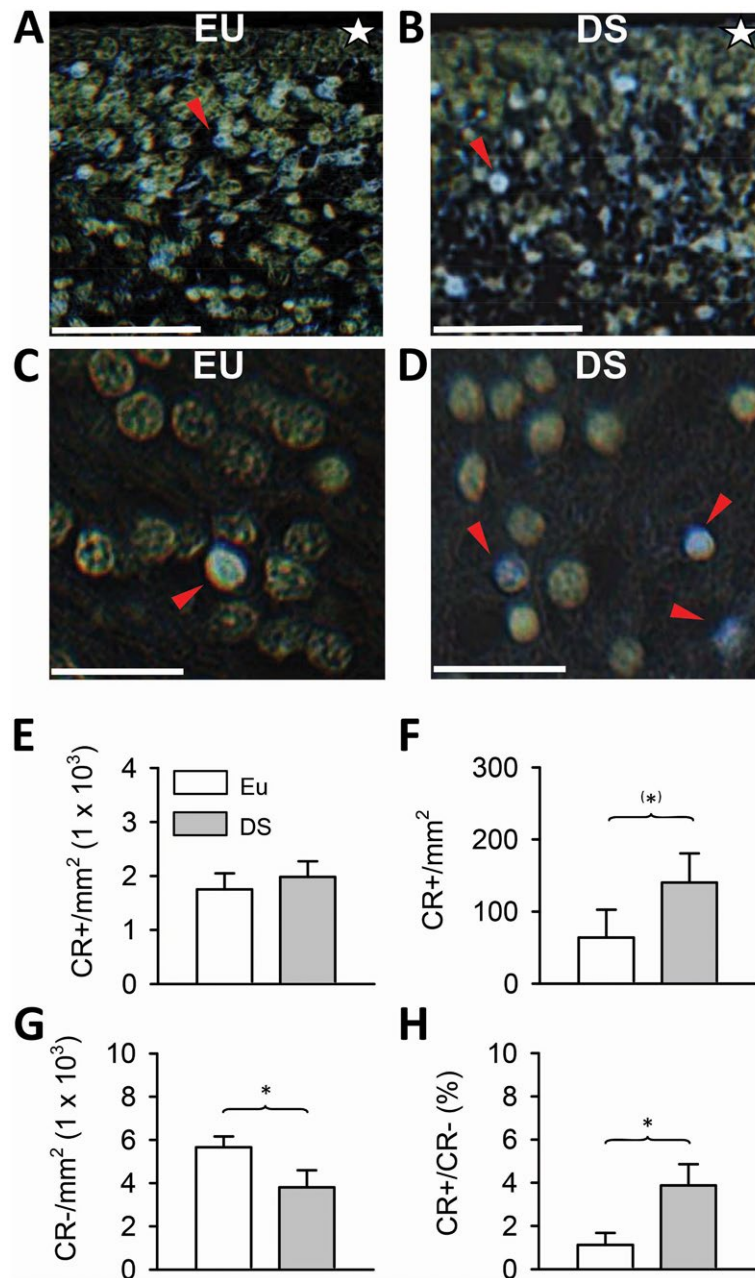
Figure 4. *Density of calretinin-positive cells in the subiculum and subicular ventricular zone in euploid fetuses and fetuses with DS.* A–D. Examples of calretinin-positive cells in the ventricular zone (A) and pyramidal layer (C) of the subiculum of a euploid fetus (case 118), and in the ventricular zone (B), and pyramidal layer (D) of the subiculum of a fetus with DS (case 203). Sections were immunostained for calretinin and counterstained with hematoxylin. Colors have been inverted in order to better show calretinin-positive cells (blue cells indicated by red arrowheads). The white star in (A) and (B) indicates the border of the ventricular zone facing the ventricle. Calibration bar: A, B = 50 μM; C, D = 20 μM. E. Density of calretinin-positive cells in the ventricular zone of the subiculum. F–H. Density of calretinin-positive cells (F), calretinin-negative cells (G) and ratio of calretinin-positive over calretinin-negative cells (H) in the subiculum of fetuses with DS (n = 3) and euploid fetuses (n = 3). Values are mean ± SD. (*)$P < 0.06$; *$P < 0.05$ (two tailed t-test). Abbreviations: CR = calretinin; DS = Down syndrome; EU = euploid.

were astrocytes or had an undetermined phenotype. Confirming previous evidence, fetuses with DS had a reduced percentage of neurons and an increased percentage of astrocytes in comparison with euploid fetuses (14,15). Thus, not only has the VZ of the subiculum of fetuses with DS fewer progenitor cells, but these cells appear to be impaired in their differentiation program. Within the nervous system, neurons represent crucial constituents because they are the
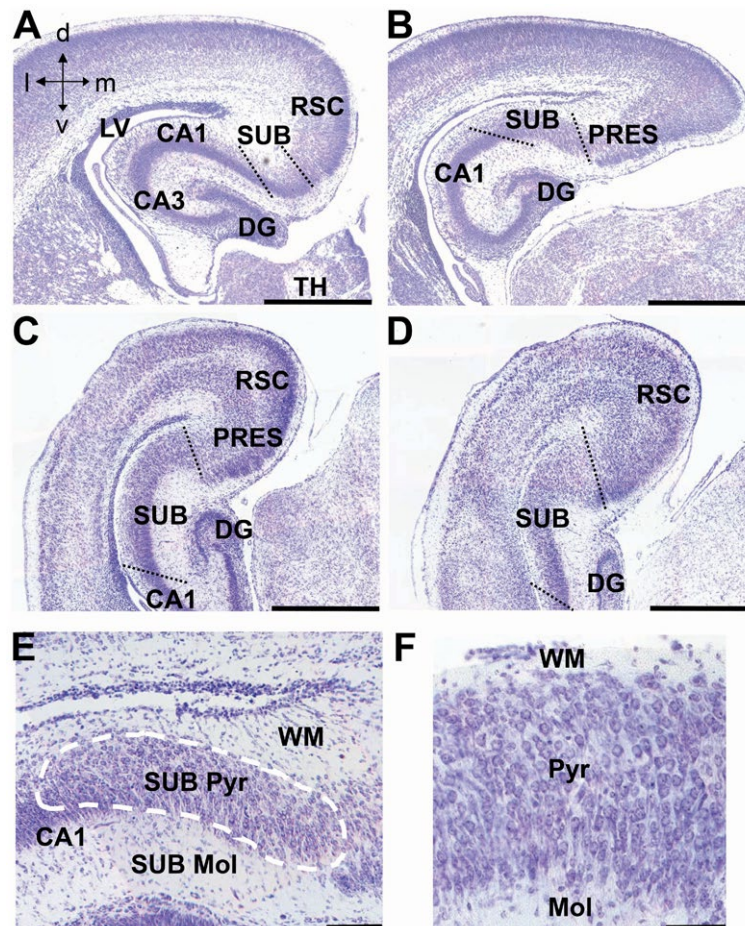
Figure 5. *Anatomy of the subiculum in neonate mice.* **A–D.** Nissl-stained coronal sections across the subiculum of a euploid mouse aged 2 days. Sections in (**A–D**) show the subiculum at progressively more caudal levels going from (**A**) to (**D**). The dotted lines indicate the border of the subiculum with field CA1 and cortical areas. **E, F.** Higher magnification images showing the layers (**E**) and cytoarchitecture (**F**) of the subiculum. The dashed line in (**E**) encloses the pyramidal layer of the subiculum. Calibration bar: **A–D** = 500 µM; **E** = 100 µM; **F** = 50 µM. Abbreviations: CA1 and CA3 = hippocampal fields; d = dorsal; DG = dentate gyrus; l = lateral; LV = lateral ventricle; m = medial; Mol = molecular layer; PRES = presubiculum; Pyr = pyramidal layer; RSC = retrosplenial cortex; SUB = subiculum; TH = thalamus; v = ventral; WM = white matter.

only cells that can communicate signals in a fast way and for long distances. Thus, the reduced density of neurons in the subiculum of fetuses with DS implies poor connections with the remaining parts of the brain. Interestingly, at mid-gestation, a projection from field CA1 to the entorhinal cortex and a parallel projection from the subiculum have been detected. These projections are reciprocated by projections from the entorhinal cortex (19). This evidence appears of relevance for two reasons. First, it shows that the connections between the subiculum, CA1, and entorhinal cortex, that have been shown to be fundamental for memory retrieval in rodents, are already present in the human fetal brain (22,30). Second, the poor cellularity found here in the subiculum of fetuses with DS suggests an alteration of these relationships starting from early phases of brain development. This precocious alteration may be a key factor leading to the functional alterations in recall memory in children (and adults) with DS.

The subiculum of fetuses with DS exhibits an increased percentage of calretinin-positive cells

Cortical GABAergic interneurons can be subdivided into three populations based on the expression of parvalbumin, calbindin, and calretinin (CR). In primates, CR-positive neurons are the most abundant interneuronal population (20). Unlike other calcium-binding proteins, CR is expressed early in neocortical development [see (4)]. An evaluation of the density of CR-positive cells in the pyramidal layer of the subiculum showed that it was notably smaller than that of CR-negative cells. As discussed above, most of these cells are neurons and much fewer cells are astrocytes. A comparison of fetuses with DS and euploid fetuses showed that the subiculum of fetuses with DS had a larger density of CR-positive cells in comparison with euploid fetuses, a significantly reduced density of CR-negative cells, and an increased ratio of CR-positive vs. CR-negative cells. This evidence shows that fetuses with DS have
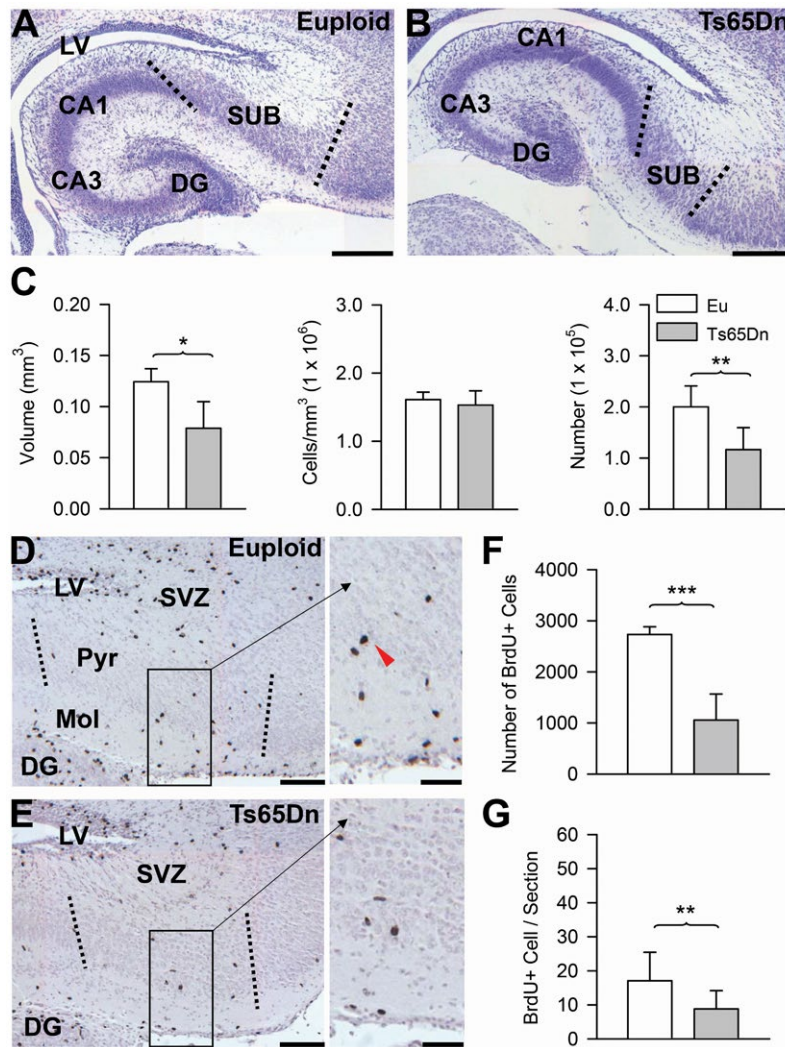
Figure 6. *Cellularity and proliferation rate in the subiculum of Ts65Dn and euploid mice.* **A–B.** Nissl-stained coronal sections across the subiculum of a euploid (**A**) and a Ts65Dn (**B**) mouse aged two days. Images, which were taken at approximately the same rostro-caudal plane, show that the size of the subiculum is patently reduced in Ts65Dn mice. The dotted lines indicate the borders of the subiculum with field CA1 and the cortex. Calibration bar: **A**, **B** = 200 μM. **C.** Volume of the pyramidal layer of the subiculum (panel on the left), cell density (middle panel) and total number of cells (panel on the right) in the pyramidal layer of the subiculum of euploid (n = 5) and Ts65Dn (n = 5) mice. Values (mean ± SD) refer to one hemisphere. **D, E.** Sections immunostained for BrdU and counterstained with hematoxylin across the subiculum of a euploid (**D**) and a Ts65Dn (**E**) mouse. The dotted lines indicate the borders of the subiculum. Higher magnification images of the boxed areas are reported on the right. The red arrowhead shows a BrdU-positive cell. Calibration bar = 100 μM (higher magnification images); 50 μM (lower magnification images). **F, G.** Total number of BrdU-positive cells (upper panel) and mean number of BrdU-positive cells per section (lower panel) in the pyramidal layer plus molecular layer of the subiculum in euploid (n = 5) and Ts65Dn (n = 5) mice. Values (mean ± SD) refer to on hemisphere. *$P < 0.05$; **$P < 0.01$ (two tailed *t*-test). Abbreviations: CA1, CA3 = hippocampal fields; DG = dentate gyrus; Eu = euploid; LV = lateral ventricle; Pyr = pyramidal layer; Mol = molecular layer; SUB = subiculum; SVZ = subventricular zone.

proportionally more CR-positive interneurons than euploid fetuses. In the human forebrain, neurons are generated during a restricted period that begins at approximately GW 6 and is largely completed by week 18 (32). Thus, in most brain regions, the asset of principal neurons and interneurons present at mid-gestation is likely to represent the template of the future cellular organization of those regions. Most of CR-positive cells in the human cortex

are GABAergic (3). It is well established that GABA exerts inhibitory effects at adult life stages. GABAergic transmission, however, exerts depolarizing instead of hyperpolarizing effects at early stages of brain development (5). While the role of CR-positive cells in the fetal brain remains to be identified, the current finding that fetuses with DS have a proportionally larger density of CR-positive cells in comparison with euploid fetuses suggests that this

imbalance may translate in an excitation–inhibition imbalance at postnatal life stages.

Unlike the principal neurons of the cortex that originate in the VZ, the inhibitory interneurons derive from the medial and caudal ganglionic eminences (3,13). The ganglionic eminences, however, are not the sole site of origin of interneurons, because CR-positive cells have been detected in the fetal VZ of the neocortex (21,36). Our findings are in full agreement with this observation and additionally show that CR-positive cells are also present in the VZ of the hippocampal region. A comparison of euploid fetuses and fetuses with DS showed no differences in the density of CR-positive neurons in the VZ of the subiculum. This suggests no impairment in the proliferation potency of the progenitors of this interneuron population. Previous evidence showed that in Ts65Dn embryos the progenitors of inhibitory interneurons, unlike those of excitatory neurons, exhibit an increase in proliferation potency in comparison with euploid mice (10,11). Although we did not found an increase in the density of CR-positive cells in the VZ of fetuses with DS, our findings are in line with those obtained in the Ts65Dn model because they show that the neurogenesis impairment that characterizes the DS fetal brain is not shared by the progenitors of CR-positive interneurons.

Developmental alterations of the subiculum in the Ts65Dn mouse

Mice are very immature at birth and, unlike in humans, their nervous system considerably develops postnatally. In the current study, we found that the subiculum of neonate Ts65Dn mice is notably hypotrophic, in terms of overall volume and cellularity, in comparison with that of euploid mice. This finding, which complements previous evidence regarding the hippocampus and dentate gyrus of Ts65Dn mice (16), suggests that hypotrophy is a feature that is shared by various structures of the hippocampal region. While the rostral VZ/SVZ of the forebrain gives origin to neurons (and glia) destined to the rostral forebrain, the caudal VZ/SVZ gives origin to neurons (and glia) destined to the caudal parts of the forebrain, including the hippocampal region (7). The reduced number of cells populating the subiculum found here can be accounted for the reduced proliferation potency that characterizes the caudal SVZ (16).

Consistently with the reduced proliferation potency exhibited by the caudal SVZ of Ts65Dn mice, we found here that in the subiculum of Ts65Dn mice, there were fewer BrdU-positive cells. The fate of these cells remains to be established, although most of the cells from the perinatal SVZ appear to give origin to astrocytes and oligodendrocytes (7). The finding that most of the BrdU-positive cells in the subiculum of neonate mice were in the molecular layer, a layer that contains numerous nerve fibers, suggests that these cells may be precursors of oligodendrocytes. If so, the reduced number of BrdU-positive cells in the subiculum of Ts65Dn mice may lead to myelination impairment, a feature that characterizes the trisomic brain (1,26).

Conclusions

This study shows numerous developmental defects in the subiculum of fetuses with DS. These defects are in line with similar defects previously found in other structures of the hippocampal region and in the ventral temporal cortex (14,15). Taken together, our studies suggest widespread damage of the memory systems of temporal lobe in the DS brain starting from fetal life stages. These neuroanatomical alterations, in turn, may account for the alterations in several domains of explicit memory exhibited by children with DS (8,24,33). In view of the emerging role of the subiculum in memory retrieval, the developmental defects found here in the subiculum of fetuses with DS may account for the impairment in recall memory found in children with DS (9).

The subiculum of the Ts65Dn mouse exhibits neuroanatomical defects resembling those seen in human fetuses with DS. A number of studies has examined the anatomy and function of the hippocampus in this mouse model but no study has taken into consideration the subiculum. Our study may prompt further investigations aimed at characterizing the electrophysiology of the subicular circuits. This may help deciphering the possible electrophysiological basis of DS-linked alterations in the subicular function. Among the numerous mouse models of DS, no perfect mouse model currently exists (18). In spite of some limitations, the Ts65Dn mouse is the more widely used model of DS. In order to establish the "quality" of a disease model, it is important to obtain as much comparative information as possible regarding the phenotypic features of the human disease and the chosen model. The Ts65Dn mouse exhibits a number of brain phenotypic features that closely resemble those seen in individual with DS. The current study, by providing comparative information regarding the subicular neuroanatomy in fetuses with DS and in the Ts65Dn model, adds a piece of information to the characterization of the Ts65Dn mouse. An increase in the body of evidence regarding the phenotypic resemblance between individuals with DS and the Ts65Dn model is of relevance in the field of preclinical studies on DS, because this knowledge may increase the confidence that results obtained in this model can be transferred to the human condition.

CONFLICT OF INTEREST

Authors report no conflict of interest.

REFERENCES

1. Abraham H, Vincze A, Veszpremi B, Kravjak A, Gomori E, Kovacs GG, Seress L (2011) Impaired myelination of the human hippocampal formation in Down syndrome. *Int J Dev Neurosci* **30**:147–158.

2. Arnold SE, Trojanowski JQ (1996) Human fetal hippocampal development: I. Cytoarchitecture, myeloarchitecture, and neuronal morphologic features. *J Comp Neurol* **367**:274–292.

3. Barinka F, Druga R (2010) Calretinin expression in the mammalian neocortex: a review. *Physiol Res* **59**:665–677.

4. Bayatti N, Moss JA, Sun L, Ambrose P, Ward JF, Lindsay S, Clowry GJ (2008) A molecular neuroanatomical study of the developing human neocortex from 8 to 17 postconceptional weeks revealing the early differentiation of the subplate and subventricular zone. *Cereb Cortex* **18**:1536–1548.

5. Ben-Ari Y, Khalilov I, Represa A, Gozlan H (2004) Interneurons set the tune of developing networks. *Trends in neurosciences* **27**:422–427.

6. Bianchi P, Ciani E, Guidi S, Trazzi S, Felice D, Grossi G *et al* (2010) Early pharmacotherapy restores neurogenesis and cognitive performance in the Ts65Dn mouse model for Down syndrome. *J Neurosci* **30**:8769–8779.

7. Brazel CY, Romanko MJ, Rothstein RP, Levison SW (2003) Roles of the mammalian subventricular zone in brain development. *Prog Neurobiol* **69**:49–69.

8. Carlesimo GA, Marotta L, Vicari S (1997) Long-term memory in mental retardation: evidence for a specific impairment in subjects with Down's syndrome. *Neuropsychologia* **35**:71–79.

9. Carr VA, Rissman J, Wagner AD (2010) Imaging the human medial temporal lobe with high-resolution fMRI. *Neuron* **65**:298–308.

10. Chakrabarti L, Best TK, Cramer NP, Carney RS, Isaac JT, Galdzicki Z, Haydar TF (2010) Olig1 and Olig2 triplication causes developmental brain defects in Down syndrome. *Nat Neurosci* **13**:927–934.

11. Chakrabarti L, Galdzicki Z, Haydar TF (2007) Defects in embryonic neurogenesis and initial synapse formation in the forebrain of the Ts65Dn mouse model of Down syndrome. *J Neurosci* **27**:11483–11495.

12. Contestabile A, Fila T, Ceccarelli C, Bonasoni P, Bonapace L, Santini D *et al* (2007) Cell cycle alteration and decreased cell proliferation in the hippocampal dentate gyrus and in the neocortical germinal matrix of fetuses with Down syndrome and in Ts65Dn mice. *Hippocampus* **17**:665–678.

13. Gonzalez-Gomez M, Meyer G (2014) Dynamic expression of calretinin in embryonic and early fetal human cortex. *Front Neuroanat* **8**:41.

14. Guidi S, Bonasoni P, Ceccarelli C, Santini D, Gualtieri F, Ciani E, Bartesaghi R (2008) Neurogenesis impairment and increased cell death reduce total neuron number in the hippocampal region of fetuses with Down syndrome. *Brain Pathol* **18**:180–197.

15. Guidi S, Emili M, Giacomini A, Stagni F, Bartesaghi R (2017) Neuroanatomical alterations in the temporal cortex of human fetuses with Down syndrome. 2nd International Conference of the Trisomy 21 Research Society, June 7–11, 2017, Chicago, USA, #24, p. 79.

16. Guidi S, Stagni F, Bianchi P, Ciani E, Giacomini A, De Franceschi M *et al* (2014) Prenatal pharmacotherapy rescues brain development in a Down's syndrome mouse model. *Brain* **137**:380–401.

17. Haydar TF, Reeves RH (2012) Trisomy 21 and early brain development. *Trends Neurosci* **35**:81–91.

18. Herault Y, Delabar JM, Fisher EMC, Tybulewicz VLJ, Yu E, Brault V (2017) Rodent models in Down syndrome research: impact and future opportunities. *Dis Model Mech* **10**:1165–1186.

19. Hevner RF, Kinney HC (1996) Reciprocal entorhinal-hippocampal connections established by human fetal midgestation. *J Comp Neurol* **372**:384–394.

20. Hladnik A, Dzaja D, Darmopil S, Jovanov-Milosevic N, Petanjek Z (2014) Spatio-temporal extension in site of origin for cortical calretinin neurons in primates. *Front Neuroanat* **8**:50.

21. Jakovcevski I, Mayer N, Zecevic N (2011) Multiple origins of human neocortical interneurons are supported by distinct expression of transcription factors. *Cereb Cortex* **21**:1771–1782.

22. Ledergerber D, Moser EI (2017) Memory retrieval: taking the route via subiculum. *Curr Biol* **27**:R1225–R1227.

23. Milojevich H, Lukowski A (2016) Recall memory in children with Down syndrome and typically developing peers matched on developmental age. *J Intellect Disabil Res* **60**:89–100.

24. Nadel L (2003) Down's syndrome: a genetic disorder in biobehavioral perspective. *Genes Brain Behav* **2**:156–166.

25. O'Mara S (2006) Controlling hippocampal output: the central role of subiculum in hippocampal information processing. *Behav Brain Res* **174**:304–312.

26. Olmos-Serrano JL, Kang HJ, Tyler WA, Silbereis JC, Cheng F, Zhu Y *et al* (2016) Down Syndrome developmental brain transcriptome reveals defective oligodendrocyte differentiation and myelination. *Neuron* **89**:1208–1222.

27. Reeves RH, Irving NG, Moran TH, Wohn A, Kitt C, Sisodia SS *et al* (1995) A mouse model for Down syndrome exhibits learning and behaviour deficits. *Nat Genet* **11**:177–184.

28. Reinholdt LG, Ding Y, Gilbert GJ, Czechanski A, Solzak JP, Roper RJ *et al* (2011) Molecular characterization of the translocation breakpoints in the Down syndrome mouse model Ts65Dn. *Mamm Genome* **22**:685–691.

29. Rose DS, Maddox PH, Brown DC (1994) Which proliferation markers for routine immunohistology? A comparison of five antibodies. *J Clin Pathol* **47**:1010–1014.

30. Roy DS, Kitamura T, Okuyama T, Ogawa SK, Sun C, Obata Y, Yoshiki A, Tonegawa S (2017) Distinct neural circuits for the formation and retrieval of episodic memories. *Cell* **170**:1000–1012.e19.

31. Seress L, Abraham H, Tornoczky T, Kosztolanyi G (2001) Cell formation in the human hippocampal formation from mid-gestation to the late postnatal period. *Neuroscience* **105**:831–843.

32. Stiles J, Jernigan TL (2010) The basics of brain development. *Neuropsychol Rev* **20**:327–348.

33. Vicari S, Bellucci S, Carlesimo GA (2000) Implicit and explicit memory: a functional dissociation in persons with Down syndrome. *Neuropsychologia* **38**:240–251.

34. West MJ, Gundersen HJ (1990) Unbiased stereological estimation of the number of neurons in the human hippocampus. *J Comp Neurol* **296**:1–22.

35. Witter MP, Canto CB, Couey JJ, Koganezawa N, O'Reilly KC (2014) Architecture of spatial circuits in the hippocampal region. *Philos Trans R Soc Lond B Biol Sci* **369**:20120515.

36. Zecevic N, Hu F, Jakovcevski I (2011) Interneurons in the developing human neocortex. *Dev Neurobiol* **71**:18–33.